S-Endoglin Expression Is Induced in Senescent Endothelial Cells and Contributes to Vascular Pathology

Francisco J. Blanco, María T. Grande, Carmen Langa, Barbara Oujo, Soraya Velasco, Alicia Rodriguez-Barbero, Eduardo Perez-Gomez, Miguel Quintanilla, Jose M. López-Novoa and Carmelo Bernabeu

Circ. Res. 2008;103;1383-1392; originally published online Oct 30, 2008;
DOI: 10.1161/CIRCRESAHA.108.176552
Circulation Research is published by the American Heart Association. 7272 Greenville Avenue, Dallas, TX 72514
 Print ISSN: 0009-7330. Online ISSN: 1524-4571

S-Endoglin Expression Is Induced in Senescent Endothelial Cells and Contributes to Vascular Pathology

Francisco J. Blanco, María T. Grande, Carmen Langa, Barbara Oujo, Soraya Velasco, Alicia Rodriguez-Barbero, Eduardo Perez-Gomez, Miguel Quintanilla, Jose M. López-Novoa, Carmelo Bernabeu

Abstract—Senescence of endothelial cells (ECs) may contribute to age-associated cardiovascular diseases, including atherosclerosis and hypertension. The functional and gene expression changes associated with cellular senescence are poorly understood. Here, we have analyzed the expression, during EC senescence, of 2 different isoforms (L, long; S, short) of endoglin, an auxiliary transforming growth factor (TGF)-β receptor involved in vascular remodeling and angiogenesis. As evidenced by RT-PCR, the S/L ratio of endoglin isoforms was increased during senescence of human ECs in vitro, as well as during aging of mice in vascularized tissues. Next, the effect of S-endoglin protein on the TGF-β receptor complex was studied. As revealed by coimmunoprecipitation assays, S-endoglin was able to interact with both TGF-β type I receptors, ALK5 and ALK1, although the interaction with ALK5 was stronger than with ALK1. S-endoglin conferred a lower proliferation rate to ECs and behaved differently from L-endoglin in relation to TGF-β–responsive reporters with ALK1 or ALK5 specificities, mimicking the behavior of the endothelial senescence markers Id1 and plasminogen activator inhibitor-1. In situ hybridization studies demonstrated the expression of S-endoglin in the endothelium from human arteries. Transgenic mice overexpressing S-endoglin in ECs showed hypertension, decreased hypertensive response to NO inhibition, decreased vasodilatory response to TGF-β_1 administration, and decreased endothelial nitric oxide synthase expression in lungs and kidneys, supporting the involvement of S-endoglin in the NO-dependent vascular homeostasis. Taken together, these results suggest that S-endoglin is induced during endothelial senescence and may contribute to age-dependent vascular pathology. **(*Circ Res*. 2008;103:1383-1392.)**

Key Words: endothelial cells ■ hypertension ■ TGF-β receptors ■ aging ■ endoglin

Cardiovascular repair mechanisms become progressively impaired with age, and advanced age is itself a significant risk factor for cardiovascular disease.[1] Defects in age-associated remodeling of the vascular wall are, in part, attributable to the declining of endothelial function.[2,3] Thus, vascular processes such as angiogenesis, nutrient trafficking, vascular repair, and homeostasis are impaired because of attenuation of endothelial cell (EC) proliferation, migration, or dilator responses. EC proliferation diminishes with age, entering in an irreversible senescent state.[4] Senescent cells undergo growth arrest in the G_1 phase and a change in morphology and metabolism. Some of the senescence-associated changes include cellular enlargement, altered response to growth factors such as transforming growth factor (TGF)-β_1, and expression of senescence-associated β-galactosidase (SA-β-gal).[5] Also, alterations in the expression and/or activity of the endothelial nitric oxide synthase (eNOS) are critical for the attenuation of the endothelium-dependent dilatory responses with age.[6,7] Unfortunately, most of the functional and gene expression changes associated with EC senescence remain largely unknown.[2,4]

TGF-β is a family of multifunctional cytokines that regulate EC growth, differentiation, migration, senescence, extracellular matrix production, and angiogenesis.[8] These functions are mediated through binding to a TGF-β–specific membrane receptor complex in ECs that contains 3 types of receptors: types I (TβRI) and II (TβRII), with cytoplasmic Ser/Thr-kinase activity[8]; and an auxiliary receptor named endoglin.[9] Two different TβRIs, named ALK5 and ALK1, have been shown to balance TGF-β signaling by regulating opposite functions in ECs.[8] Activation of the receptor complex triggers the phosphorylation by TβRI of the Smad family of proteins, which translocate to the nucleus to regulate gene expression. The activated TβRI determines the specificity of the downstream signaling. Thus, ALK5 phos-

Original received March 31, 2008; revision received October 20, 2008; accepted October 21, 2008.

From the Centro de Investigaciones Biologicas (F.J.B., C.L., C.B.), Consejo Superior de Investigaciones Cientificas, Madrid; CIBER de Enfermedades Raras (F.J.B., C.L., C.B.), Instituto de Salud Carlos III, Madrid; Instituto "Reina Sofía" de Investigación Nefrológica (M.T.G., B.O., S.V., A.R.-B, J.M.L.-N.), Departamento de Fisiologia & Farmacologia, Universidad de Salamanca and Red de Investigacion Renal; and Instituto de Investigaciones Biomedicas Alberto Sols (M.Q., E.P-G.), Consejo Superior de Investigaciones Cientificas–Universidad Autonoma de Madrid, Spain.

Correspondence to Carmelo Bernabeu, Centro de Investigaciones Biologicas, CSIC, Ramiro de Maetzu 9, 28040 Madrid, Spain. E-mail bernabeu.c@cib.csic.es

Circulation Research **is available at http://circres.ahajournals.org** **DOI: 10.1161/CIRCRESAHA.108.176552**

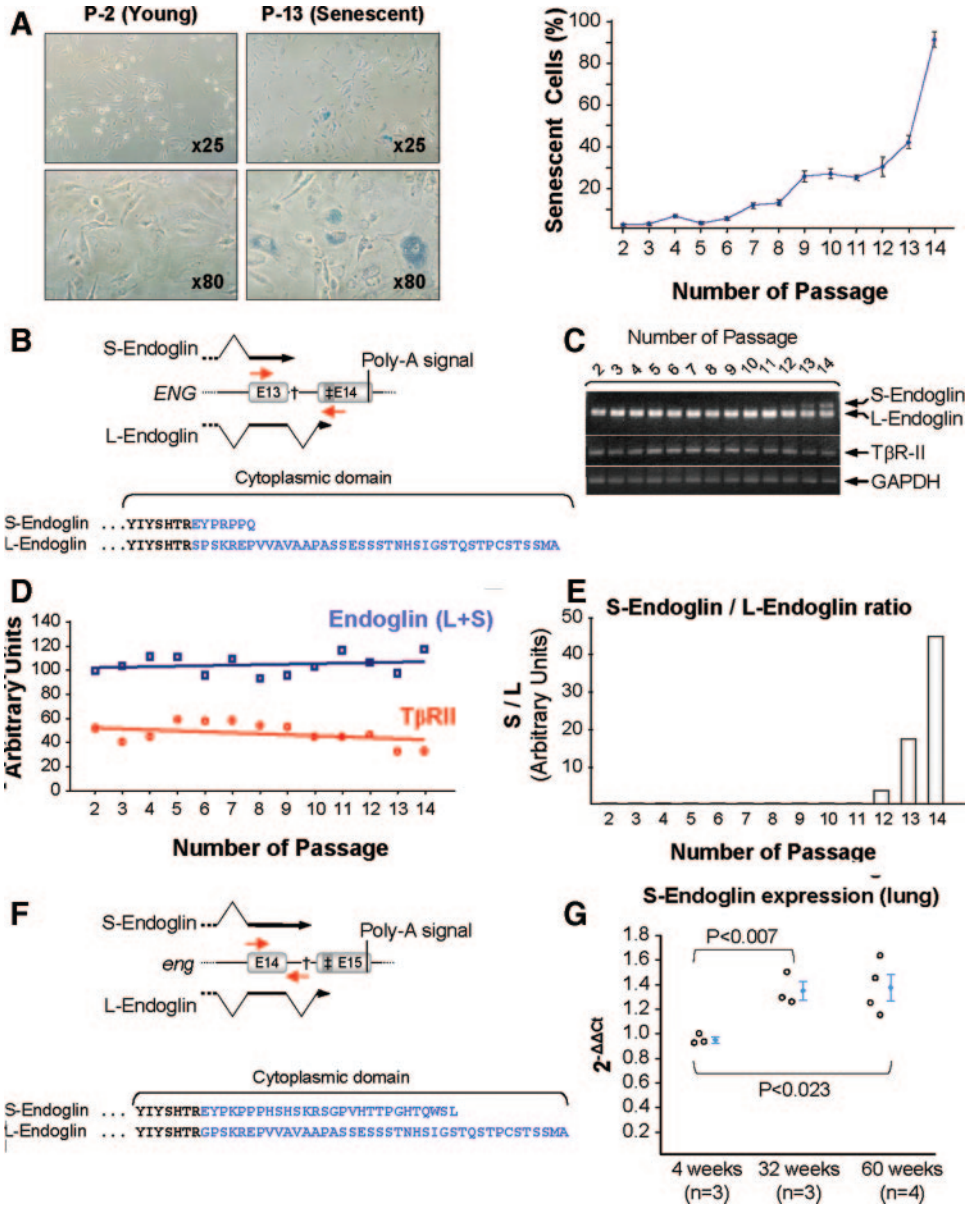

Figure 1. Effect of endothelial senescence on S-endoglin expression. A, Analysis of SA-β-gal activity in primary culture of HUVECs. Cells were seeded onto gelatin-coated plates, and passages were performed when cells achieved ≈90% confluence. Blue cytoplasmic staining is indicative of SA-β-gal activity. Representative phase contrast microscopy fields from young (second passage) and senescent (13th passage) cells are included (left). Cells positive for SA-β-gal were counted from 4 random fields, and the percentage of senescent cells was represented as the means±SEM (right). B, Schematic representation of alternative splicing in the human endoglin gene (*ENG*). A 135-bp intron between exons E13 and E14 is retained, and a premature stop codon (†) arrests translation, giving rise to S-endoglin. L-endoglin is synthesized when the same 135-bp intron is spliced and translation stops in E14 (‡). Endoglin primers that simultaneously amplify both isoforms are indicated with red arrows. Amino acid sequences from S- and L-endoglin cytoplasmic tails are shown. Sequences that differ between L and S isoforms are in blue. C through E, RT-PCR. C, Total RNA was isolated from HUVECs and submitted to semiquantitative RT-PCR using specific primers for S- and L-endoglin, TβRII, and GAPDH as an internal control. D, Total endoglin and TβRII levels. E, S-endoglin/L-endoglin ratio. F and G, Effect of aging on S-endoglin expression. F, Schematic representation of alternative splicing in mouse endoglin gene (*eng*). Primers that specifically amplify S-endoglin are indicated with red arrows. Cytoplasmic amino acid sequences that differ between L and S isoforms are in blue. G, Total RNA was isolated from lungs of mice of different ages and submitted to quantitative RT-PCR. The amount of S-endoglin amplificate ($2^{-\Delta\Delta Ct}$) was normalized to the endogenous 18S RNA. Each circle represents the mean of triplicates with an SD of <2% (n=number of animals).

phorylates Smad2/Smad3, whereas ALK1 activates Smad1/Smad5.[8]

Endoglin is a 180-kDa homodimer predominantly expressed in ECs that plays an important role in angiogenesis, vascular remodeling, and vascular pathology.[9] Mutations in endoglin and ALK1 genes are responsible for an autosomal dominant vascular dysplasia termed hereditary hemorrhagic telangiectasia, characterized by recurrent hemorrhages and cerebral, hepatic, and pulmonary arteriovenous malformations.[8] The in vivo expression of 2 different alternatively spliced isoforms, long (L)-endoglin and short (S)-endoglin, has been demonstrated in human and mouse tissues.[10–12] L-endoglin, the predominant isoform in ECs, directly interacts with ALK1, ALK5, and TβRII[13,14] and modulates EC

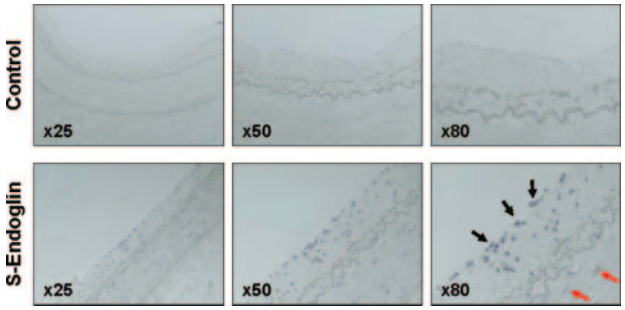

Figure 2. In situ hybridization of S-endoglin in human coronary artery. Sense (Control) and antisense S-endoglin cRNA probes were uniformly labeled with digoxigenin-UTP and hybridized to slides from human coronary artery. Riboprobes were detected with anti-digoxigenin Fab fragments conjugated to alkaline phosphatase, followed by incubation with the chromogenic substrate. No contrast staining was performed. Black arrows show the specific hybridization of S-endoglin to the endothelium, whereas red arrows indicate occasional staining of smooth muscle cells. Magnifications are indicated.

responses to TGF-β.[13,15–17] Whereas L-endoglin represses the TGF-β/ALK5/Smad3 pathway involved in plasminogen activator inhibitor (PAI)-1 expression,[18,19] it activates that of TGF-β/ALK5/Smad2 to enhance eNOS expression[20,21] and triggers the TGF-β/ALK1/Smad1 route to increase Id1 expression.[13,15] Although, the role of S-endoglin in TGF-β signaling has been recently addressed in keratinocytes[12] and myoblasts,[22] little is known about the expression and function of S-endoglin in ECs. Here, we have analyzed the enhanced expression of S-endoglin during EC senescence and the functions affected by this isoform.

Materials and Methods

Cell culture[13,19,23]; senescence-associated β-gal staining[5]; semiquantitative and quantitative RT-PCR[11,24]; in situ hybridization and expression vectors[12,14]; reporter assays[13]; transgenic mice expressing human S-endoglin in ECs (*S-Eng*$^+$ mice)[25]; transfections, immunoprecipitation, and Western blot analyses[13,20,26]; urinary nitrite measurements[20]; and radiotelemetry monitoring of blood pressure[27] are described in the expanded Materials and Methods section in the online data supplement, available online at http://circres.ahajournals.org.

Results

S-Endoglin Expression Increases in Senescent ECs

Human umbilical vein endothelial cell (HUVEC) primary cultures showed increased senescence morphology along the number of passages, as evidenced by the blue SA-β-gal activity staining of their cytoplasm (Figure 1A). The size of SA-β-gal–positive cells was significantly larger than that of SA-β-gal negative cells, as expected for senescent cells (Figure I in the online data supplement). At the 14th passage, cells stopped proliferating, in agreement with the high percentage of senescent cells. At each passage, total RNA from HUVECs was isolated and subjected to RT-PCR using specific primers to detect TβRII and endoglin transcripts (Figure 1B). Along the different passages, no significant differences were obtained in the expression levels of total endoglin or TβRII (Figure 1C and 1D). Interestingly, S-endoglin began to be expressed at the 12th passage and displayed the highest expression level at the 14th passage (Figure 1C and 1E), sharing expression with its longer counterpart in senescent cells. Next, the expression of mouse S-endoglin during endothelial senescence in vivo was assessed. As determined by quantitative RT-PCR using specific primers (Figure 1F), transcript levels of S-endoglin were significantly increased in lungs from 32- and 60-week-old mice as compared with young animals (4 weeks old) (Figure 1G). To assess whether S-endoglin is expressed by ECs in vivo, in situ hybridization experiments with human coronary arteries were carried out (Figure 2). The antisense S-endoglin–specific riboprobe clearly hybridized with the endothelium monolayer and with some ECs in the subendothelial zone and tunica media that likely belong to the network of small vessels that vascularize the large coronary artery. Some scattered smooth muscle cells were also stained in the tunica media, which is compatible with the expression of endoglin protein in smooth muscle cells from human atherosclerotic plaques.[28] As a negative control, the sense S-endoglin–specific riboprobe did not yield any signal above background levels. The endothelial labeling of S-endoglin was reproduced in human veins and lungs (supplemental Figure II).

Interaction of S-Endoglin With ALK5 and ALK1

The extracellular and cytoplasmic domains of L-endoglin contribute to the physical and functional interaction with ALK5 and ALK1.[13,14] Thus, it was of interest to investigate the behavior of S-endoglin in this context. Because both isoforms share a common extracellular domain, we assessed whether the S-endoglin cytoplasmic domain was able to physically interact with both TGF-β type I receptors. COS-7 cells were cotransfected with hemagglutinin (HA)-tagged ALK5 or ALK1 plus the HA-tagged vectors TMCT-EndoL or TMCT-EndoS, containing the transmembrane and cytoplasmic domains from L- or S-endoglin, respectively. We found that antibodies against either ALK5 or ALK1 can coimmunoprecipitate the cytoplasmic tails from both endoglin isoforms (Figure 3A). Interestingly, the amount of TMCT-EndoS or TMCT-EndoL coimmunoprecipitated with ALK5 was similar, whereas the amount of TMCT-EndoS coimmunoprecipitated with ALK1 was much lower than that of TMCT-EndoL (Figure 3C). These results suggest that the S-endoglin cytoplasmic tail interacts with ALK5 and ALK1 but shows a lower affinity for ALK1 than for ALK5. The specificity of these interactions was confirmed by using an HA-tagged irrelevant protein that yielded negative results. As a control, a Western blot analysis of the total cellular extracts is included (Figure 3B).

We next assayed the interacting ability of the full-length isoform by cotransfecting Flag-tagged S-endoglin with HA-tagged ALK5 or ALK1 in COS-7 cells. Antibodies against the Flag epitope in S-endoglin were able to coimmunoprecipitate ALK5 with high yield (Figure 4A). By contrast, the S-endoglin/ALK1 interaction appeared to be much weaker ($<$50-fold; Figure 4C). A Western blot analysis of total cellular extracts was included to monitor the recombinant protein expression (Figure 4B).

S-Endoglin and L-Endoglin Modulate the ALK5 and ALK1 Signaling Pathways Differently

The different behaviors of S-endoglin versus L-endoglin, with respect to the interaction with the type I receptors,

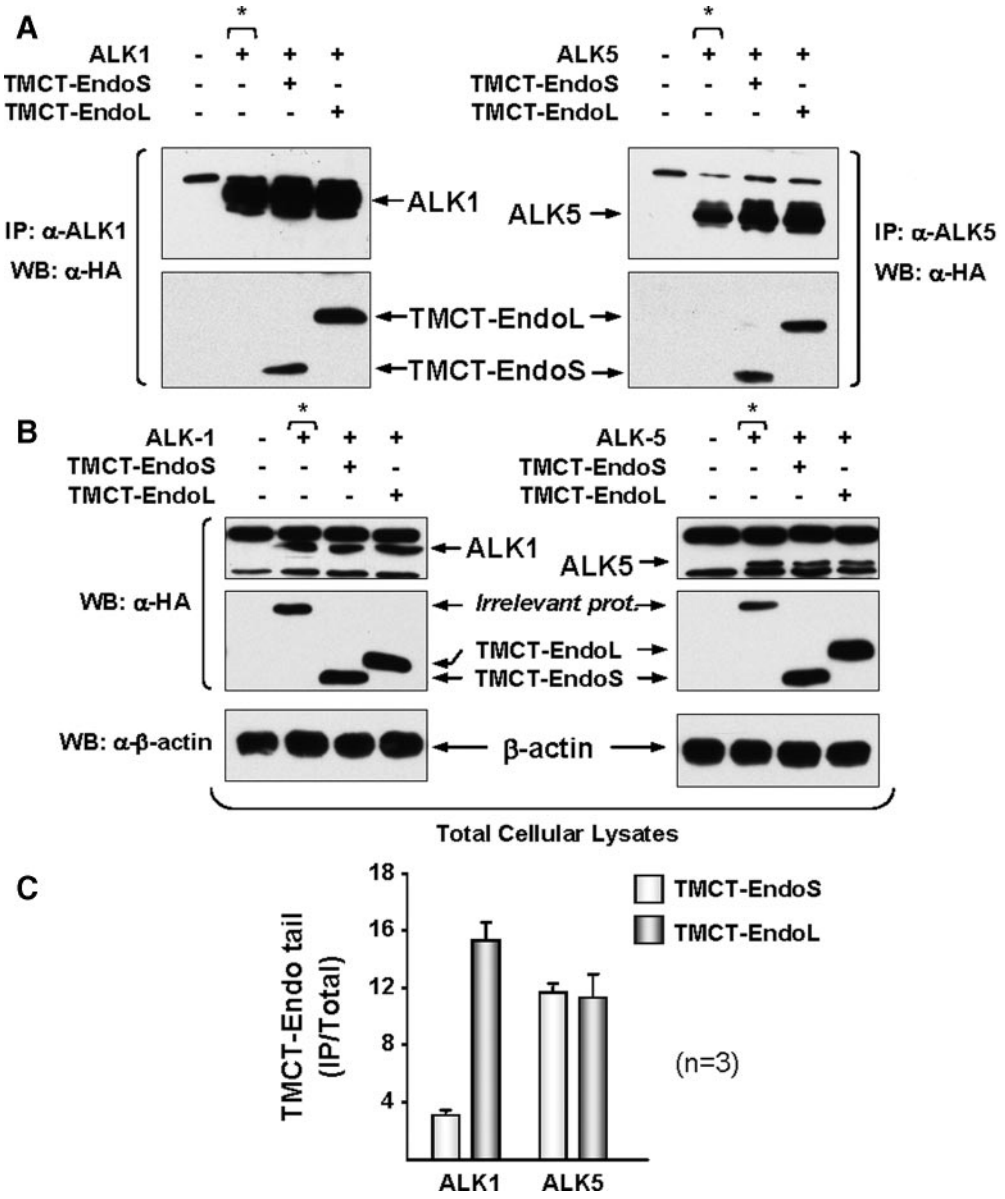

Figure 3. Interaction of S-endoglin cytoplasmic tail with ALK1 and ALK5. COS-7 cells were transiently cotransfected with HA-tagged ALK1 and ALK5 or S-endoglin (TMCT-EndoS) or L-endoglin (TMCT-EndoL) cytoplasmic tails. An irrelevant HA-tagged protein (*) was included as a control. Cell lysates were immunoprecipitated (IP) with the indicated antibodies. Immunoprecipitates (A) and total cell lysates (B) were subjected to SDS-PAGE under reducing conditions, followed by Western blot (WB) with anti-HA or anti–β-actin antibodies. Bands corresponding to the coimmunoprecipitated endoglin cytoplasmic domains were subjected to densitometry and were normalized. The mean of 3 different experiments is shown in C.

suggest a specific functional role for S-endoglin in the endothelial TGF-β system. To address this issue, ECs were transfected with S-endoglin expression vector and the effect on the ALK5/ALK1 pathways was assessed (Figure 5). In HMEC-1 cells, the presence of S-endoglin enhanced the TGF-β–induced activity of the ALK5/Smad3 specific reporter $p(CAGA)_{12}$-Luc compared with control cells (Figure 5A). In the same experiment, L-endoglin overexpression led to the inhibition of the $p(CAGA)_{12}$-Luc activity in response to TGF-β, as reported.[13] Next, the endothelial system GM7372-EL, engineered to express human L-endoglin in the presence of doxycycline,[23] was used. Again, TGF-β–induced activity of the $p(CAGA)_{12}$-Luc reporter was significantly increased on S-endoglin expression (Figure 5B). By contrast, L-endoglin expression, induced with doxycycline, not only inhibited the basal TGF-β–induced activity of the ALK5 reporter but also counteracted its S-endoglin–dependent enhancement. These results indicate that S-endoglin and L-endoglin have distinct effects on the ALK5/Smad3 signaling pathway. Because the extracellular domain is common to both endoglin variants,[11] we assessed whether the isoform-specific cytoplasmic tails were responsible for their divergent behavior. Dissection of the independent functional role of each isoform is not easy to address in ECs because these cells show high levels of the predominant L-endoglin. The parental myoblast cell line L6E9 has the advantage of providing an endoglin-free background, and stable transfectants expressing either L-endoglin or S-endoglin[19] somehow mimic the independent contribution of each isoform in young or senescent cells, respectively. Thus, myoblasts stably expressing S-endoglin or L-endoglin were transfected with TMCT-EndoL or TMCT-EndoS constructs, respectively. Ectopic expression of the cytoplasmic region of L-endoglin markedly reduced the TGF-β–induced activity of the $p(CAGA)_{12}$-Luc reporter in S-endoglin–expressing cells (Figure 5C). Conversely, the cytoplasmic region of S-endoglin clearly enhanced the TGF-β–induced activity of the same reporter in L-endoglin–expressing cells, suggesting that the modulator

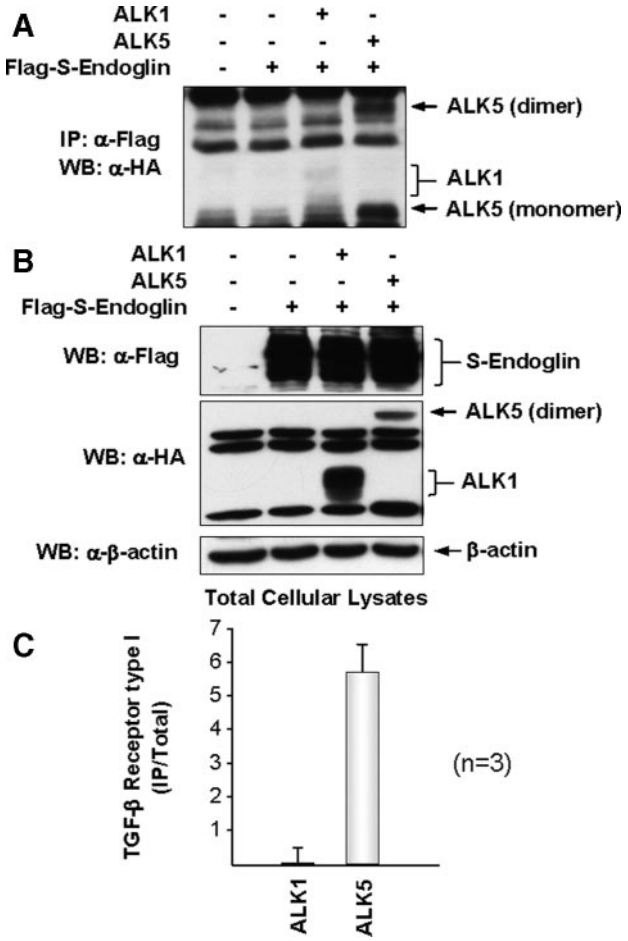

Figure 4. Interaction of full-length S-endoglin with ALK1 and ALK5. COS-7 cells were transiently cotransfected with Flag-tagged S-endoglin and HA-tagged ALK5 or ALK1. Cell lysates were immunoprecipitated with anti-Flag antibodies. Immunoprecipitates (A) and total cellular lysates (B) were subjected to SDS-PAGE under nonreducing conditions, followed by Western blot analysis. β-Actin was included as a loading control. Bands corresponding to the coimmunoprecipitated ALK1 and ALK5 were subjected to densitometry and were normalized. The mean of 3 different experiments is shown in C.

effect of endoglin isoforms on the ALK5 pathway depends on their cytoplasmic region.

The differential effect of S-endoglin versus L-endoglin was also assessed using the $p(BRE)_2$-Luc reporter vector as a sensor for the ALK1/Smad1 pathway. S-endoglin expression did not affect the basal reporter activity, whereas the presence of L-endoglin markedly induced the $p(BRE)_2$-Luc activity (Figure 5D). As expected, high doses of TGF-β_1 inhibited $p(BRE)_2$-Luc activity.

The results shown above indicate that S-endoglin and L-endoglin isoforms have distinct functional roles on the ALK5 and ALK1 signaling pathways. Because upregulation of PAI-1 and Id1 is specifically dependent on the TGF-β/ALK5 or TGF-β/ALK1 pathway, respectively,[15,29] we assessed the effect of S-endoglin on pId1-Luc and p800-Luc reporters driven by the promoters of these genes. On transfection of HMEC-1, the Id1 promoter activity, both in the absence and in the presence of TGF-β_1, decreased in response to increasing amounts of S-endoglin (Figure 5E). As a control, L-endoglin induced the transcriptional activity of pId1-Luc vector. On the other hand, increasing amounts of S-endoglin augmented in a dose-dependent fashion the activity of the PAI-1 reporter (Figure 5F). By contrast, L-endoglin inhibited the activity of PAI-1 reporter, as expected. Moreover, the effect of S-endoglin on the expression of the senescence associated markers PAI-1 and Id1,[4,30] was assessed in senescent ECs whose S-endoglin levels are upregulated (Figure 1). As shown by semiquantitative RT-PCR experiments, senescent HUVECs display higher transcript levels of PAI-1 and lower transcript levels of Id1 than control cells (Figure 5G). In the same experiment, no significant differences in the levels of ALK1 or ALK5 were observed. As expected, the transcript levels of telomerase, a marker of senescence, were clearly downregulated. To address the role of S-endoglin in EC proliferation, murine lung ECs derived from *S-Eng*$^+$ transgenic animals were analyzed. As shown in Figure 5H, *S-Eng*$^+$ ECs displayed a lower proliferation rate than ECs from wild-type animals. Because cellular senescence is associated with decreased cell proliferation, this result supports the contribution of S-endoglin to EC senescence.

Taken together, these results suggest that, at variance with L-endoglin, S-endoglin potentiates the ALK5 pathway, leading to increased PAI-1, whereas it inhibits the ALK1 route, leading to decreased Id1 expression, thus mimicking the phenotype of senescent ECs.

Hemodynamics and eNOS Expression in Transgenic Mice Expressing S-Endoglin

The prevalence of cardiovascular disease increases with age and is associated with increased arterial pressure and decreased expression and/or activity of eNOS. To address the potential contribution of S-endoglin to the vascular pathology, *S-Eng*$^+$ transgenic mice[25] were analyzed. The weight was similar for S-*Eng*$^+$ mice and control littermates (supplemental Figure III). Systolic, diastolic and mean arterial pressure values were higher in *S-Eng*$^+$ than in control littermates (Figure 6A through 6C), whereas no significant differences were observed in heart rate (Figure 6D). Because endoglin regulates the expression of eNOS and thereby the NO-dependent vascular homeostasis,[20] the role of NO was next addressed. Intravenous infusion of the nonspecific nitric oxide synthase inhibitor N^G-nitro-L-arginine methyl ester (L-NAME) increased blood pressure in both *S-Eng*$^+$ and control littermate mice (Figure 6E and 6F), while reducing the heart rate (Figure 6G). Interestingly, L-NAME infusion resulted in a smaller increase in systolic and diastolic (33% less) blood pressure in *S-Eng*$^+$ as compared with control mice (Figure 6E and 6F), suggesting less biologically available NO in the setting of *S-Eng*$^+$ overexpression. Furthermore, acetylcholine-induced hypotension, an effect that is also mediated by NO, was significantly reduced in *S-Eng*$^+$ as compared with control mice, whereas no significant differences were observed with sodium nitroprusside (an NO synthesis–independent, cGMP-dependent vasodilator) or with hydralazine (an NO synthesis–independent, cGMP-independent vasodilator) (supplemental Table II), again suggesting a lower NO production in *S-Eng*$^+$ as compared with

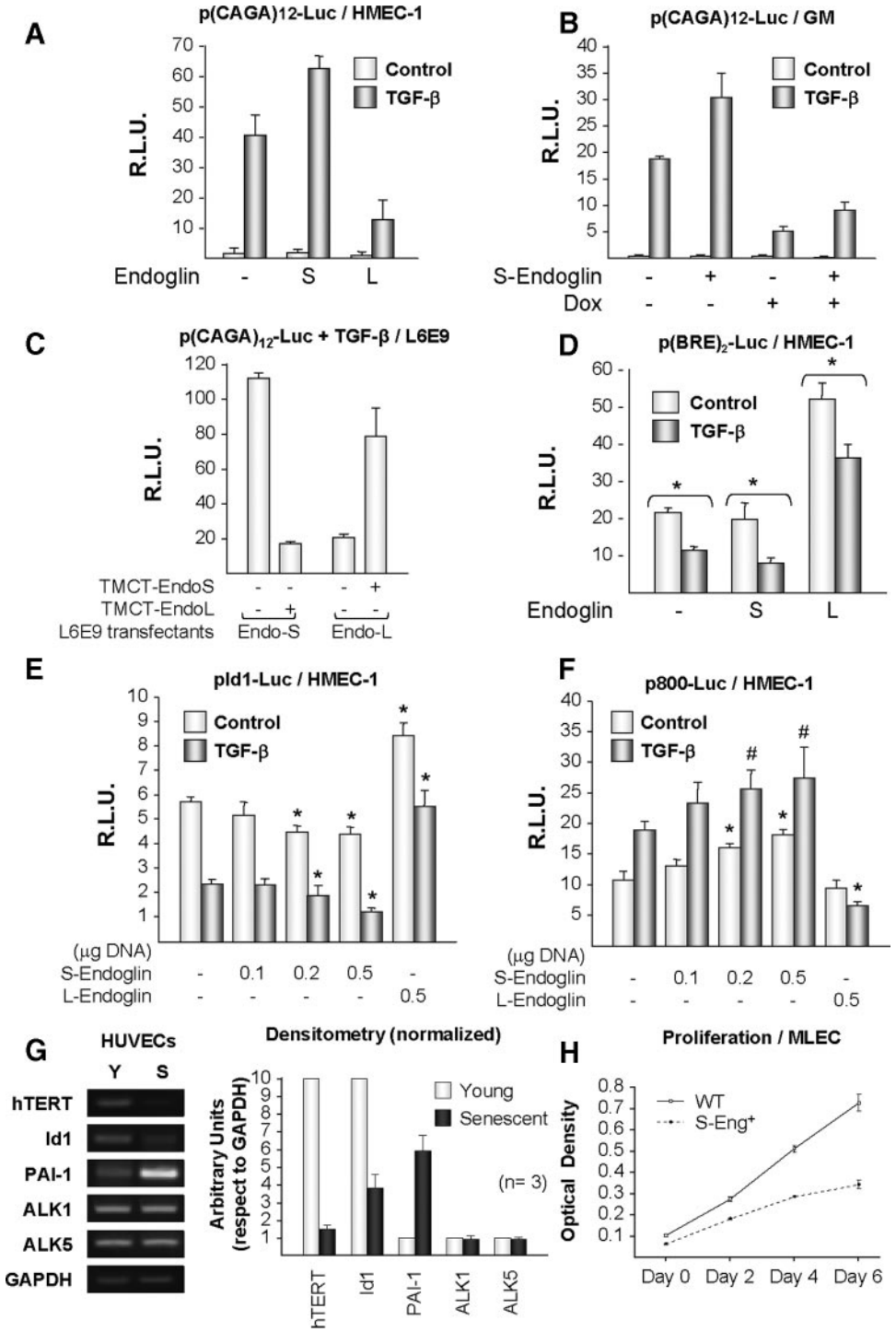

Figure 5. Effect of S-endoglin expression on ALK5 and ALK1 pathways. A, HMEC-1 cells were cotransfected with p(CAGA)$_{12}$-Luc reporter construct, S-endoglin (S), and L-endoglin (L). The luciferase activity in response to 10 ng/mL TGF-β_1 for 24 hours was measured as an indicator of the ALK5/Smad3 pathway. B, Endothelial GM7372-EL cells were cotransfected with p(CAGA)$_{12}$-Luc reporter construct and S-endoglin. Expression of L-endoglin was induced with 500 ng/mL doxycycline, and the luciferase activity in response to TGF-β_1 was determined. C, L6E9 stable transfectants for S-endoglin (Endo-S) or L-endoglin (Endo-L) were transiently cotransfected with S-endoglin (TMCT-Endo-S) or L-endoglin (TMCT-Endo-L) cytoplasmic tails, respectively, and p(CAGA)$_{12}$-Luc vector. The reporter activity in response to 10 ng/mL TGF-β_1 for 24 hours was determined. For clarity, the negligible reporter activity in the absence of TGF-β has been omitted. D, HMEC-1 cells were cotransfected with p(BRE)$_2$-Luc reporter construct, S-endoglin (S), and L-endoglin (L), as indicated. The luciferase activity was measured as an indicator of the ALK1 pathway. Significant differences were observed between TGF-β–treated and untreated cells (*$P<0.01$). E and F, Antagonistic effect of S-endoglin on the PAI-1 and Id1 promoters. HMEC-1 cells were transfected with pId1-Luc reporter vector containing the Id1 promoter, p800-Luc reporter vector containing the PAI-1 promoter, and different amounts of S-endoglin or L-endoglin expression vectors. Cells were treated or not with 10 ng/mL TGF-β_1 for 24 hours, and the luciferase activity was determined. Significant differences were observed between endoglin-transfected and control cells. *$P<0.01$, #$P<0.05$. G, Effect of endothelial senescence on Id1 and PAI-1 expression. Total RNA was isolated from young (Y) (third

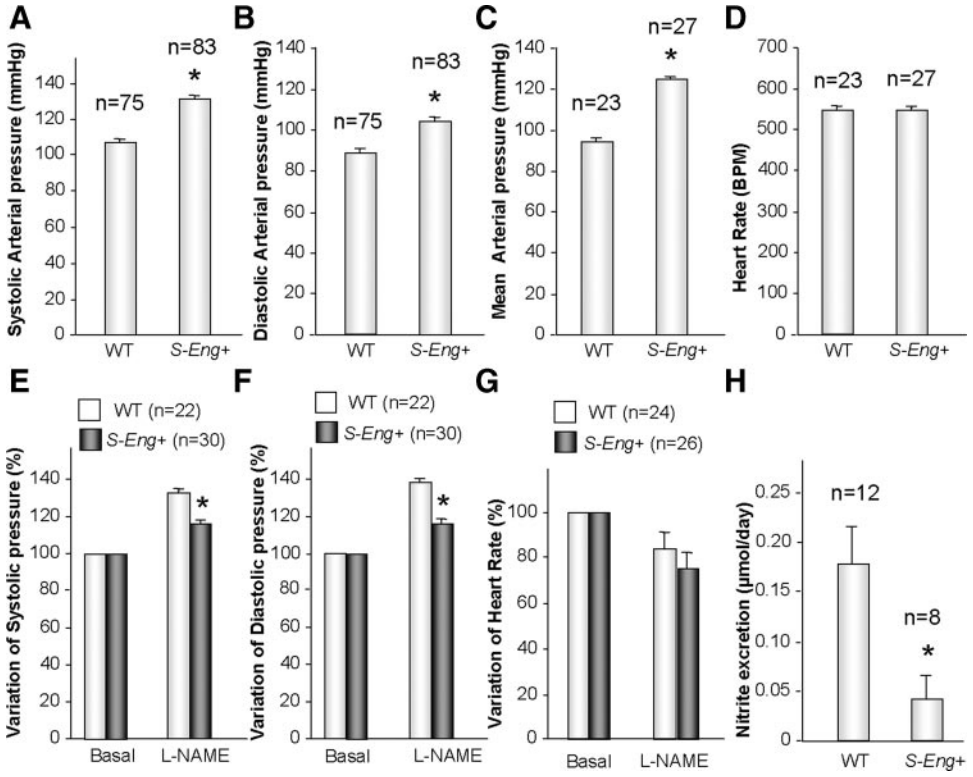

Figure 6. Arterial pressure in *S-Eng*$^+$ mice. A through D, Systolic (A), diastolic (B), and mean arterial (C) pressures were measured by radiotelemetry in *S-Eng*$^+$ and control mice. The heart rate was also measured (D). E through G, Effect of NO synthesis inhibition. Variation of systolic pressure (E), diastolic pressure (F), and heart rate (G) were measured in *S-Eng*$^+$ and control mice intraperitoneally infused or not with L-NAME. Arbitrary values of 100 were assigned to untreated animals. H, NO synthesis. Concentration of nitrites in urine was determined. Significant differences were observed between *S-Eng*$^+$ and control mice (*$P<0.01$).

control mice. In fact, lower urinary nitrite excretion in *S-Eng*$^+$ mice compared with control littermates was observed (Figure 6H), thus reflecting a reduced renal NO synthesis. In addition, eNOS expression was significantly lower, whereas cyclooxygenase (COX)-2 expression was significantly higher, in either kidney or lungs of *S-Eng*$^+$ mice compared with control littermates (Figure 7A and 7B). Because TGF-β_1 leads to an increased vasodilatation in *Eng*$^{+/+}$ mice that is severely impaired in *Eng*$^{+/-}$ mice,[21] the possible involvement of S-endoglin in the TGF-β-regulated vascular homeostasis was addressed next. *S-Eng*$^+$ mice and control littermates showed a decrease in arterial pressure (diastolic and systolic) after TGF-β_1 injection, but the decrease was significantly lower in *S-Eng*$^+$ mice than in control littermates (Figure 7C and 7D). As a control, no significant differences were observed in the effects of TGF-β_1 on heart rate between *S-Eng*$^+$ mice and control littermates (Figure 7E).

Discussion

Senescence of endothelial cells plays a critical role in cardiovascular diseases that are associated with aging. However, the underlying molecular mechanisms that involve the senescent ECs are poorly understood. Here, we report, for the first time, that expression of S-endoglin is induced during senescence of ECs (Figure 8). We provide evidence that in vivo and in vitro expression of S-endoglin contributes to the cardiovascular pathology associated with age, although a limitation of this study is the lack of functional analysis on blocking S-endoglin. Our present data support that upregulation of S-endoglin expression is part of the senescent program of ECs rather than being the sole responsible for senescence.

To date, most of the studies on endoglin have focused on the predominant L-endoglin isoform, although significant levels of S-endoglin mRNA are coexpressed with L-endoglin in vivo.[11,12] These isoforms are generated by alternative splicing, and the only difference between human S-endoglin and L-endoglin transcripts is an intronic sequence of 135-bp that is retained in S-endoglin.[11] Unfortunately, no consensus small interfering RNA motifs could be identified in this sequence. Consequently, the analysis of functional effects of S-endoglin silencing is not feasible, and this represents a technical limitation of this study. On the other hand,

passage) or senescent (S) (13th passage) HUVECs as in Figure 1. Samples were subjected to RT-PCR using specific primers (supplemental Table I) for Id1, PAI-1, ALK1, ALK5, human telomerase reverse transcriptase (hTERT), and GAPDH as an internal control. Transcript levels were normalized with respect to GAPDH, giving an arbitrary value of 10 (Id1, hTERT) or 1 (PAI-1, ALK1, ALK5) to young HUVECs. Densitometry of 3 different experiments was carried out, and the means±SEM is shown. H, Effect of S-endoglin expression on cellular proliferation. Pools from primary lung ECs from 3 S-*Eng*$^+$ or 3 wild-type (WT) mice were plated, and, at the times indicated, proliferation was assessed using an MTT assay by measuring the optical density at 570 nm. Each data point is the mean of triplicate samples. This is a representative experiment out of 4 different experiments using MTT or crystal violet staining.

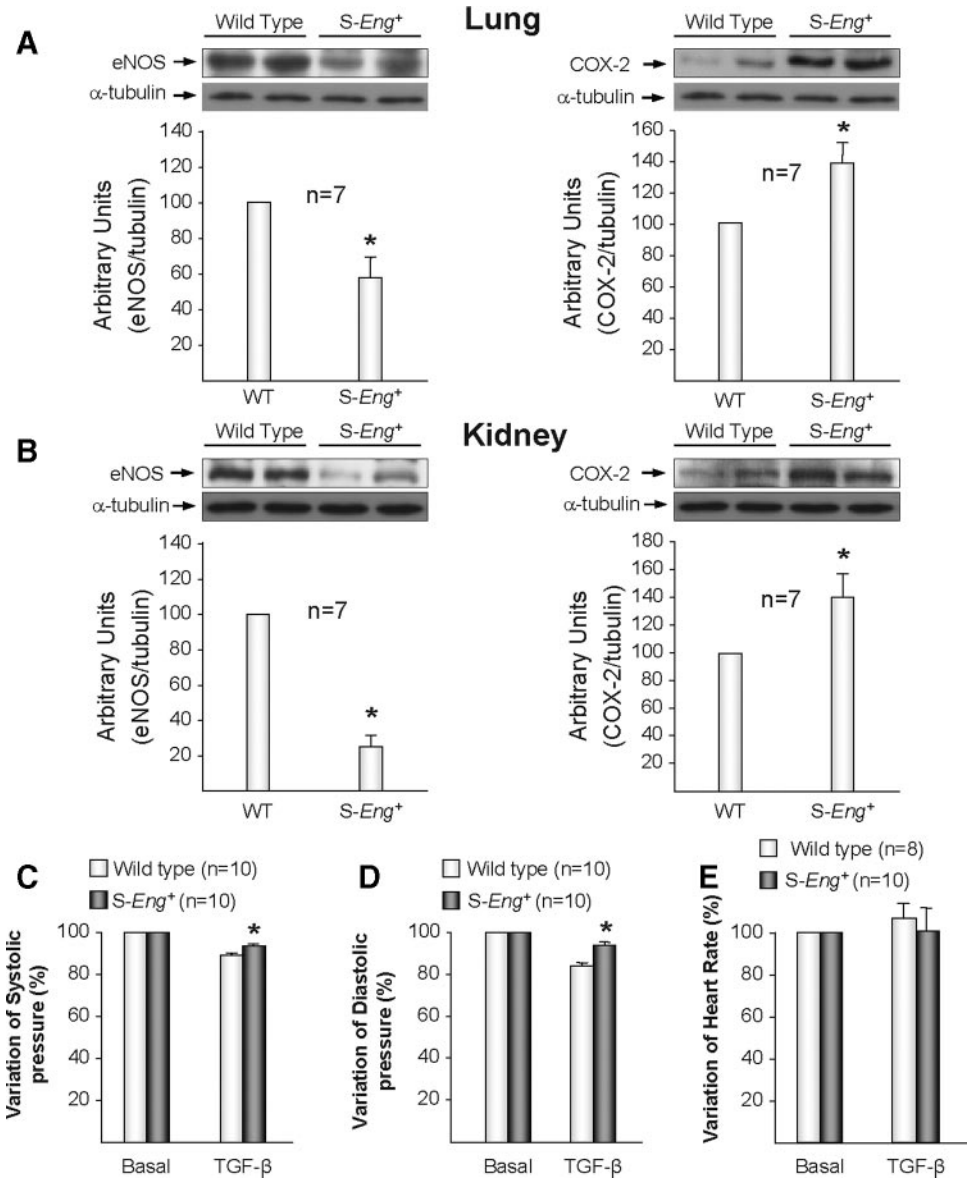

Figure 7. Endoglin-dependent vascular homeostasis in *S-Eng*$^+$ mice. A and B, Expression of eNOS and COX-2 in lungs (A) and kidneys (B), as determined by Western blot. Significant differences were observed between *S-Eng*$^+$ and wild-type mice (*$P<0.01$). C through E, Effect of TGF-β. Variation of systolic pressure (C), diastolic pressure (D), and heart rate (E) were measured in mice infused or not with TGF-β_1. Arbitrary values of 100 were assigned to untreated animals. *Significant differences ($P<0.01$) with respect to wild-type animals.

S-endoglin and L-endoglin proteins vary from each other in their cytoplasmic tails that contain 14 and 47 amino acids, respectively, with a sequence of only 7 residues being specific for S-endoglin. This small structural difference explains the lack of appropriate tools to clearly distinguish between L-endoglin and S-endoglin in tissues and primary cultured cells. Thus, analysis by ectopic expression of cDNAs encoding human L- and S-endoglin in cell transfectants and transgenic mice represents an excellent model system to understand the role of these isoforms. In this study, we demonstrate that the functional role of L-endoglin is different from that of S-endoglin in ECs. This comparative study has been addressed by analyzing the TGF-β signaling pathway in ECs, where the TGF-β type I receptors ALK1 and ALK5 appear to play an active role in regulating the activation/resolution phases of angiogenesis.[8,15] We show that S-endoglin interacts with both ALK5 and ALK1, although the interaction with ALK5 was stronger than with ALK1. This is at variance with L-endoglin that shows a higher affinity for ALK1 versus ALK5.[13] Because the extracellular domain of endoglin is common in both isoforms, their cytoplasmic tails appear to be responsible for these differences. Thus, whereas ALK5 interacts with both endoglin cytoplasmic tails with comparable affinity, the interaction between ALK1 and the cytoplasmic tail of S-endoglin was significantly lower than with the long counterpart. Moreover, S-endoglin behaved differently than L-endoglin in relation to several TGF-β-responsive reporters with different specificities. Thus, S-endoglin expression increases the ALK5 signaling pathway, whereas L-endoglin inhibits the same pathway in ECs.

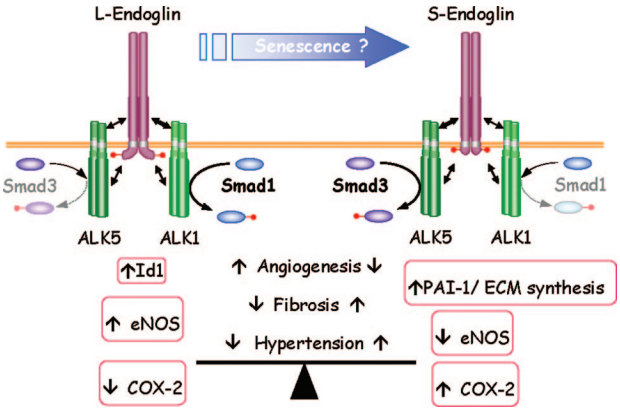

Figure 8. Hypothetical model of S-endoglin functions during senescence. In the normal state, the TGF-β response is modulated by L-endoglin, but, on senescence of ECs, S-endoglin is upregulated, interacting with the TGF-β receptor complex containing ALK1 and ALK5. As a consequence of this interaction, S-endoglin regulates the expression of different TGF-β target genes including PAI-1, Id1, eNOS, and COX-2. Thus, S-endoglin allows a switch that triggers the cardiovascular pathology: (1) upregulation of PAI-1/extracellular matrix (ECM) synthesis may lead to increased fibrosis; (2) downregulation of Id1 is associated with decreased angiogenesis; and (3) downregulation of eNOS and upregulation of COX-2 are involved in hypertension. The involvement of TβRII, TGF-β, and S-endoglin/L-endoglin heterodimers has been omitted for simplification.

Interestingly, S-endoglin also favors ALK5/Smad3 signaling in mouse carcinoma cells and rat myoblasts.[22,24] On the other hand, L-endoglin, but not S-endoglin, stimulated the ALK1 signaling pathway. These results are in agreement with reports showing that L-endoglin promotes endothelial cell proliferation via TGF-β/ALK1 signaling, whereas it interferes with the TGF-β/ALK5 pathway,[9,13,15] and suggest that S-endoglin acts as an antagonist of L-endoglin. In fact, S-endoglin appears to have a negative effect on EC proliferation. This is compatible with the reported antiangiogenic effect of S-endoglin in contrast to the proangiogenic role attributed to L-endoglin.[12,26,31] Interestingly, angiogenic function is progressively impaired with increasing age,[32] which fits well with the upregulation of S-endoglin in senescent ECs and its antiangiogenic effect. This short endoglin isoform is able to exert opposite effects to that of the predominantly expressed L-endoglin on the TGF-β signal, including the positive and negative cooperation with ALK5 and ALK1, respectively. Because both endoglin isoforms are coexpressed in senescent ECs, this raises the question about the molecular mechanism by which L-endoglin and S-endoglin antagonize with each other. The reported heterodimeric association between S-endoglin and L-endoglin[12] could possibly account for a mutually interfering effect. Of note, ALK5 and ALK1 levels are not significantly altered between young and senescent ECs. This suggests that the S-endoglin/L-endoglin ratio in ECs may contribute to balancing the TGF-β signal through ALK5 or ALK1 and their important roles in vascular pathophysiology.[8] In this context, increased synthesis of extracellular matrix is a pathological process widely related to high circulating levels of TGF-β and with the activation of the ALK5/Smad3 signaling pathway.[33,34] Whereas S-endoglin highly increased the ALK5 signaling pathway, L-endoglin inhibited the same route, in agreement with a number of reports describing the role of L-endoglin as an antagonist of ALK5-mediated TGF-β induction of extracellular matrix synthesis.[18,19,35] The positive contribution of S-endoglin to the profibrotic TGF-β/ALK5 pathway suggests its involvement in the increased fibrosis associated with vascular senescence.[36]

Further support for the involvement of S-endoglin in the cardiovascular pathology associated with senescence was obtained using S-endoglin transgenic animals. *S-Eng*$^+$ mice show hypertension, a defective hypertensive response to the inhibition of NO synthesis with L-NAME, and a decreased urinary nitrite excretion, thus suggesting a defective NO synthesis. This interpretation is supported by the decreased eNOS expression in lungs and kidneys of these animals, as well as the positive relationship between levels of L-endoglin and eNOS reported in both mice and cultured ECs.[20,26] In addition, endoglin-deficient mice show a defective endothelium-dependent vasorelaxation and decreased NO production,[20] similarly to S-endoglin transgenic mice. Of note, NO inhibits EC senescence,[37] thus supporting the involvement of S-endoglin in this process. Furthermore, in both cultured ECs and endoglin-deficient mice, low levels of L-endoglin are associated with high COX-2 expression,[26] a correlation also found in S-*Eng*$^+$ mice. Thus, in vivo overexpression of S-endoglin appears to result in the same phenotype as L-endoglin deficiency, suggesting opposing functional effects of both isoforms on the NO and COX-2 systems. On the other hand, *S-Eng*$^+$ transgenic mice also show a reduced hypotensive response to TGF-β_1 administration, in agreement with the finding that TGF-β_1 regulates eNOS expression[38] and induces vasodilatation in wild-type mice, which is severely impaired in endoglin-deficient animals.[21] Thus, S-endoglin seems to have the opposite behavior than L-endoglin in these vascular parameters.

Taken together, these findings suggest that the alternatively spliced S-endoglin contributes to the cardiovascular pathology associated with aging. Further studies on the triggering mechanisms that control the alternative splicing of endoglin gene will help to better understand the genetic and physiological programs under which S-endoglin exert its function.

Acknowledgments

We acknowledge the technical assistance of Annette Düwel in the care and genotyping of the *S-Eng*$^+$ mice.

Sources of Funding

This work was supported by Ministerio de Ciencia e Innovacion grants SAF2007-61827 (to C.B.), SAF2007-63893 (to J.M.L.-N.), and SAF2007-63821 (to M.Q.); Junta de Castilla y Leon grant SA001/C05 (to J.M.L.-N.); CIBER de Enfermedades Raras, ISCIII-CB06/07/0038 (to C.B.); Red de Investigacion en Enfermedades Renales, ISCIII-RD06/0016 (to J.M.L.-N.); and support from the European Regional Development Fund to the Cardiovascular phenotyping unit, which includes the telemetry equipment. F.J.B. is a CIBER de Enfermedades Raras postdoctoral researcher.

Disclosures

None.

References

1. Ferrari AU, Radaelli A, Centola M. Aging and the cardiovascular system. *J Appl Physiol*. 2003;95:2591–2597.
2. Brandes RP, Fleming I, Busse R. Endothelial aging. *Cardiovasc Res*. 2005;66:286–294.
3. Minamino T, Komuro I. Vascular cell senescence: contribution to atherosclerosis. *Circ Res*. 2007;100:15–26.
4. Foreman KE, Tang J. Molecular mechanisms of replicative senescence in endothelial cells. *Exp Gerontol*. 2003;38:1251–1257.
5. Dimri GP, Lee X, Basile G, Acosta M, Scott G, Roskelley C, Medrano EE, Linskens M, Rubelj I, Pereira-Smith O. A biomarker that identifies senescent human cells in culture and in aging skin in vivo. *Proc Natl Acad Sci U S A*. 1995;92:9363–9367.
6. Sato I, Morita I, Kaji K, Ikeda M, Nagao M, Murota S. Reduction of nitric oxide producing activity associated with in vitro aging in cultured human umbilical vein endothelial cell. *Biochem Biophys Res Commun*. 1993; 195:1070–1076.
7. Förstermann U, Münzel T. Endothelial nitric oxide synthase in vascular disease: from marvel to menace. *Circulation*. 2006;113:1708–1714.
8. ten Dijke P, Arthur HM. Extracellular control of TGFbeta signalling in vascular development and disease. *Nat Rev Mol Cell Biol*. 2007;8: 857–869.
9. Bernabeu C, Conley BA, Vary CP. Novel biochemical pathways of endoglin in vascular cell physiology. *J Cell Biochem*. 2007;102: 1375–1388.
10. Gougos A, Letarte M. Primary structure of endoglin, an RGD-containing glycoprotein of human endothelial cells. *J Biol Chem*. 1990;265: 8361–8364.
11. Bellon T, Corbi A, Lastres P, Cales C, Cebrian M, Vera S, Cheifetz S, Massague J, Letarte M, Bernabeu C. Identification and expression of two forms of the human transforming growth factor-beta-binding protein endoglin with distinct cytoplasmic regions. *Eur J Immunol*. 1993;23: 2340–2345.
12. Perez-Gomez E, Eleno N, Lopez-Novoa JM, Ramirez JR, Velasco B, Letarte M, Bernabeu C, Quintanilla M. Characterization of murine S-endoglin isoform and its effects on tumor development. *Oncogene*. 2005;24:4450–4461.
13. Blanco FJ, Santibanez JF, Guerrero-Esteo M, Langa C, Vary CP, Bernabeu C. Interaction and functional interplay between endoglin and ALK-1, two components of the endothelial transforming growth factor-beta receptor complex. *J Cell Physiol*. 2005;204:574–584.
14. Guerrero-Esteo M, Sanchez-Elsner T, Letamendia A, Bernabeu C. Extracellular and cytoplasmic domains of endoglin interact with the transforming growth factor-beta receptors I and II. *J Biol Chem*. 2002;277: 29197–29209.
15. Lebrin F, Goumans MJ, Jonker L, Carvalho RL, Valdimarsdottir G, Thorikay M, Mummery C, Arthur HM, ten Dijke P. Endoglin promotes endothelial cell proliferation and TGF-beta/ALK1 signal transduction. *EMBO J*. 2004;23:4018–4028.
16. Li C, Hampson IN, Hampson L, Kumar P, Bernabeu C, Kumar S. CD105 antagonizes the inhibitory signaling of transforming growth factor beta1 on human vascular endothelial cells. *FASEB J*. 2000;14:55–64.
17. Li C, Issa R, Kumar P, Hampson IN, Lopez-Novoa JM, Bernabeu C, Kumar S. CD105 prevents apoptosis in hypoxic endothelial cells. *J Cell Sci*. 2003;116:2677–2685.
18. Guo B, Slevin M, Li C, Parameshwar S, Liu D, Kumar P, Bernabeu C, Kumar S. CD105 inhibits transforming growth factor-beta-Smad3 signalling. *Anticancer Res*. 2004;24:1337–1345.
19. Letamendia A, Lastres P, Botella LM, Raab U, Langa C, Velasco B, Attisano L, Bernabeu C. Role of endoglin in cellular responses to transforming growth factor-beta. A comparative study with betaglycan. *J Biol Chem*. 1998;273:33011–33019.
20. Jerkic M, Rivas-Elena JV, Prieto M, Carron R, Sanz-Rodriguez F, Perez-Barriocanal F, Rodriguez-Barbero A, Bernabeu C, Lopez-Novoa JM. Endoglin regulates nitric oxide-dependent vasodilatation. *FASEB J*. 2004; 18:609–611.
21. Santibanez JF, Letamendia A, Perez-Barriocanal F, Silvestri C, Saura M, Vary CP, Lopez-Novoa JM, Attisano L, Bernabeu C. Endoglin increases eNOS expression by modulating Smad2 protein levels and Smad2-dependent TGF-beta signaling. *J Cell Physiol*. 2007;210:456–468.
22. Velasco S, Alvarez-Munoz P, Pericacho M, Dijke PT, Bernabeu C, Lopez-Novoa JM, Rodriguez-Barbero A. L- and S-endoglin differentially modulate TGF-beta1 signaling mediated by ALK1 and ALK5 in L6E9 myoblasts. *J Cell Sci*. 2008;121:913–919.
23. Conley BA, Koleva R, Smith JD, Kacer D, Zhang D, Bernabeu C, Vary CP. Endoglin controls cell migration and composition of focal adhesions: function of the cytosolic domain. *J Biol Chem*. 2004;279:27440–27449.
24. Perez-Gomez E, Villa-Morales M, Santos J, Fernandez-Piqueras J, Gamallo C, Dotor J, Bernabeu C, Quintanilla M. A role for endoglin as a suppressor of malignancy during mouse skin carcinogenesis. *Cancer Res*. 2007;67:10268–10277.
25. Velasco B, Ramirez JR, Relloso M, Li C, Kumar S, Lopez-Bote JP, Perez-Barriocanal F, Lopez-Novoa JM, Cowan PJ, d'Apice AJ, Bernabeu C. Vascular gene transfer driven by endoglin and ICAM-2 endothelial-specific promoters. *Gene Ther*. 2001;8:897–904.
26. Jerkic M, Rivas-Elena JV, Santibanez JF, Prieto M, Rodriguez-Barbero A, Perez-Barriocanal F, Pericacho M, Arevalo M, Vary CP, Letarte M, Bernabeu C, Lopez-Novoa JM. Endoglin regulates cyclooxygenase-2 expression and activity. *Circ Res*. 2006;99:248–256.
27. Whitesall SE, Hoff JB, Vollmer AP, D'Alecy LG. Comparison of simultaneous measurement of mouse systolic arterial blood pressure by radiotelemetry and tail-cuff methods. *Am J Physiol Heart Circ Physiol*. 2004; 286:H2408–H2415.
28. Conley BA, Smith JD, Guerrero-Esteo M, Bernabeu C, Vary CP. Endoglin, a TGF-beta receptor-associated protein, is expressed by smooth muscle cells in human atherosclerotic plaques. *Atherosclerosis*. 2000;153: 323–335.
29. Ota T, Fujii M, Sugizaki T, Ishii M, Miyazawa K, Aburatani H, Miyazono K. Targets of transcriptional regulation by two distinct type I receptors for transforming growth factor-beta in human umbilical vein endothelial cells. *J Cell Physiol*. 2002;193:299–318.
30. Comi P, Chiaramonte R, Maier JA. Senescence-dependent regulation of type 1 plasminogen activator inhibitor in human vascular endothelial cells. *Exp Cell Res*. 1995;219:304–308.
31. Duwel A, Eleno N, Jerkic M, Arevalo M, Bolanos JP, Bernabeu C, Lopez-Novoa JM. Reduced tumor growth and angiogenesis in endoglin-haploinsufficient mice. *Tumour Biol*. 2007;28:1–8.
32. Ballard VL, Edelberg JM. Targets for regulating angiogenesis in the ageing endothelium. *Expert Opin Ther Targets*. 2007;11:1385–1399.
33. Gauldie J, Bonniaud P, Sime P, Ask K, Kolb M. TGF-beta, Smad3 and the process of progressive fibrosis. *Biochem Soc Trans*. 2007;35: 661–664.
34. Leask A, Abraham DJ. TGF-beta signaling and the fibrotic response. *FASEB J*. 2004;18:816–827.
35. Diez-Marques L, Ortega-Velazquez R, Langa C, Rodriguez-Barbero A, Lopez-Novoa JM, Lamas S, Bernabeu C. Expression of endoglin in human mesangial cells: modulation of extracellular matrix synthesis. *Biochim Biophys Acta*. 2002;1587:36–44.
36. Dao HH, Essalihi R, Bouvet C, Moreau P. Evolution and modulation of age-related medial elastocalcinosis: impact on large artery stiffness and isolated systolic hypertension. *Cardiovasc Res*. 2005;66:307–317.
37. Hayashi T, Matsui-Hirai H, Miyazaki-Akita A, Fukatsu A, Funami J, Ding QF, Kamalanathan S, Hattori Y, Ignarro LJ, Iguchi A. Endothelial cellular senescence is inhibited by nitric oxide: implications in atherosclerosis associated with menopause and diabetes. *Proc Natl Acad Sci U S A*. 2006;103:17018–17023.
38. Saura M, Zaragoza C, Cao W, Bao C, Rodriguez-Puyol M, Rodriguez-Puyol D, Lowenstein CJ. Smad2 mediates transforming growth factor-beta induction of endothelial nitric oxide synthase expression. *Circ Res*. 2002;91:806–813.

SUPPLEMENT MATERIAL

S-ENDOGLIN EXPRESSION IS INDUCED IN SENESCENT ENDOTHELIAL CELLS AND CONTRIBUTES TO VASCULAR PATHOLOGY

Francisco J. Blanco, María T. Grande, Carmen Langa, Barbara Oujo, Soraya Velasco, Alicia Rodriguez-Barbero, Eduardo Pérez-Gómez, Miguel Quintanilla, Jose M. López-Novoa, and Carmelo Bernabeu

From the Centro de Investigaciones Biológicas (F.J.B., C.L., C.B.), Consejo Superior de Investigaciones Científicas (CSIC), Madrid; Centro de Investigación Biomédica en Red de Enfermedades Raras (CIBERER) (F.J.B., C.L., C.B.) ISCIII, Madrid; Instituto "Reina Sofía" de Investigación Nefrológica (M.T.G., B.O., S.V., A.R-B, AJ.M.L-N), Departamento de Fisiología & Farmacología, Universidad de Salamanca, and Red de Investigación Renal (RedinRen); and Instituto de Investigaciones Biomédicas Alberto Sols (M.Q., E.P-G), CSIC-Universidad Autónoma de Madrid (UAM), SPAIN

Correspondence to: Carmelo Bernabeu, Centro de Investigaciones Biológicas, CSIC, Ramiro de Maetzu 9, 28040 Madrid, Spain, e-mail: bernabeu.c@cib.csic.es

EXPANDED MATERIALS AND METHODS

Cell culture

The green monkey kidney fibroblast-like cell line COS-7 and the tetracycline-inducible bovine endothelial cell line GM7372-EL were cultured in DMEM and α-MEM media (Gibco, Scotland, UK), respectively[1,2]. The L-Endoglin and S-Endoglin stable transfectants of the rat skeletal myoblast L6E9 cell line were obtained and maintained as described[3]. Culture media were supplemented with 10% heat-inactivated fetal calf serum (FCS), 2 mmol/L L-glutamine, and 100 U/mL penicillin/streptomycin. For induction of human L-Endoglin expression in GM7372-EL cells, different concentrations (20–500 ng/mL) of doxycycline (Dox; Sigma, St. Louis, MO) were used in the culture media. The human microvascular endothelial cell line HMEC-1[4] and primary cultures of human umbilical vein endothelial cells (HUVECs) were maintained in EBM-2 plus EGM-2 SingleQuots (Cambrex, Walkersville, MD). These cells were seeded and grown on plates pre-coated with 0.2% gelatin type B from bovine skin (Sigma, St. Louis, MO) in PBS. Cells were maintained in a NAPCO incubator at 37ºC in a humidified atmosphere with 5% CO_2. When required, cells were incubated with TGF-β1 (R&D Systems, Abingdon, UK).

Primary lung endothelial-cell isolation

Lungs from *S-Eng*$^+$ transgenic mice or normal littermates *S-Eng*$^-$ were minced, collagenase-digested (Gibco Invitrogen), sieved through a 70 µm-pore size cell strainer (BD Falcon), and the cell suspension was seeded on plates precoated with 0.1% gelatin (Sigma), 10 µg/mL fibronectin (Sigma), and 30 µg/mL Vitrogen (BD Biosciences) in PBS. Endothelial cells were purified by a single negative (FCγ-RII/III antibody; BD Pharmingen) and two positive (ICAM-2; BD Pharmingen) cell sorts using anti-rat IgG-conjugated magnetic beads (Dynal, Invitrogen). Cells were cultured routinely in a 50:50 mixture of Ham's F-12:DMEM media supplemented with 20% FCS, endothelial cell mitogen (Sigma), heparin (Sigma), and antibiotics in plates precoated as described above.

Proliferation Assays

Primary mouse lung endothelial cells were seeded onto precoated 96-well culture plates at 1,000 cells/well, and proliferation was assessed using 3-(4,5-dimethylthiazol-2-yl)-2,5 diphenyltetrazolium (MTT; Roche) over 6 days. The MTT metabolic product (formazan) was resuspended in DMSO and the optical density was measured at 570 nm. Samples were also analyzed by crystal violet staining. Cells were fixed in paraformaldeyde at defined time points and subsequently stained with crystal violet. After cell lysis with acetic acid 10%, optical density was measured at 595 nm.

Senescence Associated β-Galactosidase Activity Staining

HUVECs were cultured in 60 mm diameter gelatin pre-coated dishes. The senescence associated β-galactosidase (SA-β-gal) activity staining was performed as reported[5]. Briefly, at the indicated passage (from 2^{nd} to 14^{th}), cells were washed twice with PBS and fixed with 3.5% formaldehyde solution (Merck, Germany) in PBS for 5 minutes at room temperature. Next, dishes were washed twice and incubated at 37ºC in the absence of CO_2 during 16 hours with fresh staining solution containing 1 mg/mL 5-bromo-4-chloro-3-indolyl-β-D-galactopyranoside (X-gal), 40 mmol/L citric acid/Na_2HPO_4 buffer (pH 6.0), 5 mmol/L $K_4Fe(CN)_6$, 5 mmol/L $K_3Fe(CN)_6$, 2 mmol/L $MgCl_2$ and 150 mmol/L NaCl. The stained cells were observed with a phase contrast Axiovert 25 inverted microscope (Zeiss, Germany). The SA-β-gal activity was revealed as a blue coloured cytoplasm and the number of cells with SA-β-gal activity was determined as a mean of four random fields.

RT-PCR

For semiquantitative RT-PCR, total RNA from HUVECs was obtained using the TRIzol Reagent (Invitrogen, Scotland, UK) according to the manufacturer's instructions. The isolated RNA was resuspended in TE buffer (10 mmol/L Tris-HCl, 1 mmol/L EDTA, pH 8.0). Then, cDNA synthesis from 1 μg of total RNA was performed in 20 μL with the First Strand cDNA Synthesis kit for RT-PCR (AMV; Roche Diagnostic, Germany) using an oligo$(dT)_{15}$ primer,

following the commercial recommendations. Five μL of fresh cDNA was subjected to PCR amplification using the HotMaster Taq DNA Polymerase kit (Eppendorf, Germany). PCR products were resolved by agarose gel electrophoresis. Transcripts of human Endoglin ALK1, ALK5, TβRII, telomerase reverse transcriptase (hTERT) and glyceraldehyde-3-phosphate dehydrogenase (GAPDH), as control, were amplified using specific primers (Online Table I). S-Endoglin was detected as a 285-bp band, whereas L-Endoglin was identified as a 150-bp band[6]. Gels were documented in a Gel Doc XR System (Bio-Rad, Hercules, CA) and bands were quantified using the Quantity One software.

For quantitative RT-PCR, mouse tissue RNA was obtained using Tripure reagent (Roche, Mannheim, Germany). The determination of the transcript levels was performed by quantification assays on the basis of real-time RT-PCR with a LightCycler instrument (Roche Diagnostic, Penzberg, Germany) using fluorescence resonance energy-transfer (FRET) hybridization methodology. The gene encoding the 18S RNA was used as an internal control of the RNA quality and amplification. Primers used to amplify mouse Endoglin[7] or 18S RNAs are indicated in online Table I. The hybridization probes were designed by TibMolBiol (Berlin, Germany). Reactions for real-time PCR were performed using the one-step LightCycler kit (Roche). Four hundred ng of total cellular RNA from each tissue sample were used to generate cDNA in a reaction containing 3.25 mmol/L of $Mn(OAc)_2$, 0.5 μmol/L of each primer, 0.2 μmol/L of each probe and 1 x LC RNA Master Hybridization Probes mix (Roche). The cDNAs of Endoglin and 18S were subsequently co-amplified using the following PCR conditions: 95ºC for 2 min followed by 40 cycles with 95ºC for 10 s, 55ºC for 30 s and 72ºC for 15s. All PCR reactions were repeated for each sample in three independent experiments. Endoglin expression levels were calculated with the LightCycler Relative Quantification software (Roche).

In situ hybridization

To detect human S-Endoglin specific mRNA,[6] the intronic sequence of ENG gene flanked by part of exons #13 and #14 was amplified by PCR using the primers pair 5'-

CTCATCGGGGCCCTGCTC-3' and 5'-TGCTGCTCTCCGAGGAGG-3', and cloned using the TA Cloning kit Dual Promoter (Invitrogen). Sense control and antisense S-Endoglin cRNA probes (of ~250 nt) were uniformly labeled with digoxigenin-UTP using DIG RNA Labeling Kit Sp6/T7 (Roche), precipitated, and resuspended in hybridization buffer (50% deionized formamide, 2% Blocking Reagent from Roche, 5x SSC, 1 mg/ml total yeast tRNA, 0.1% Tween-20, 0.1% CHAPS, and 5 mM EDTA pH 8). Paraffin embedded slides from human coronary artery, vein, and lungs were purchased from Gentaur (Brussels, Belgium). Slides were deparaffinized in xylene, rehydrated, and postfixed. The sections were digested with proteinase K, treated with 2% glycine, washed and hybridized overnight at 65°C. Next, slides were washed at 65°C in 50% formamide, 2x SSC, and then at room temperature in PBST (PBS, 0.1% Tween-20). Slides were incubated with blocking buffer (2% Blocking Reagent from Roche, and 10% heat inactivated fetal calf serum in PBST) for 1 hour at room temperature. Hybridized riboprobes were detected with anti-digoxigenin Fab fragments conjugated with alkaline phosphatase (Roche) and the specific signal was revealed with a mixture of nitroblue tetrazolium chloride and 5-bromo-4-chloro-3-indolyl phosphate p-toluidine salt (NBT/BCIP solution, Roche), according to the manufacturer's instructions. Slides were visualized and photographed using an Axiovert 25 inverted microscope (Zeiss, Germany).

Expression Vectors and Transfections

Expression vectors encoding the HA-tagged truncated versions of human Endoglin TMCT-Endo-L and TMCT-Endo-S in pDisplay (Invitrogen) were generated as described[8]. TMCT-Endo-L and TMCT-Endo-S contain the transmembrane and cytoplasmic domains of L- and S-Endoglin, respectively. The expression vector pcDNA3-Endo-S encoding the Flag-tagged full-length human Endoglin-S has been reported[9]. HA-tagged expression vector encoding wild type ALK1 in pcDNA3-HASL plasmid was provided by Dr. K. Miyazono (University of Tokyo, Japan). The HA-tagged wild type ALK5 in pCMV5 was supplied by Dr. L. Attisano (University of Toronto, Canada).

Cell transfections were carried out with SuperFect Reagent (Qiagen), according to the manufacturer's instructions. Alternatively, a household cationic liposome containing 3 beta [N(N',N-dimethylaminoethane) carbamoyl] cholesterol (DC-chol) and dioleoylphosphatidylethanolamine (DOPE) (Sigma) was used. Briefly, a 20x concentrated stock solution of DC-chol:DOPE was prepared dissolving 10µl of each one in 1 mL of 37ºC warmed ethanol. The mixture was homogenized with the help of a 25G syringe and then incubated for 10 minutes at 37ºC. The working solution was prepared immediately before transfection in sterile water and filtered through 0.2 µm (Sartorius). The DNA (µg):reagent (µL) ratio was optimized to 1:5 for all experiments.

Reporter Assays

Reporter assays with TGF-β-responsive promoter constructs were performed by transient transfection as described[1], using the ALK5/Smad3 specific p$(CAGA)_{12}$-Luc[10], the ALK1/Smad1/5/8 specific p$(BRE)_2$-Luc[11], p800-Luc, containing the PAI-1 promoter[12] and pId1-Luc, containing the Id1 promoter[13] vectors in the presence or absence of TGF-β1. Relative luciferase units were determined in a TD20/20 luminometer (Promega, Madison, WI). Samples were co-transfected with the SV40-β-galactosidase expression plasmid as an internal control to correct for transfection efficiency. Measurement of β-galactosidase activity was performed using the Galacto-Ligth kit (Tropix). The experiments were performed in triplicate at least three times and representative experiments are shown in the figures.

Immunoprecipitation and Western-blot analyses

Transfected cells were lysed at 4ºC for 30 minutes with lysis buffer (50 mmol/L pH 7.4 HEPES, 150 mmol/L NaCl, 100 µmol/L EGTA, 500 µmol/L EDTA, 10 mmol/L NaF, 1 mmol/L Na_3VO_4, 10% digitonin, 10% glycerol and a mixture of protease inhibitors (Complete, Roche). Aliquots of total cell lysates were subjected to SDS-PAGE and electrotransferred to a PVDF membrane for specific immunodetection. For immunoprecipitation studies, aliquots of total cell lysates containing equal amounts of total protein were pre-cleared for 4 hours with protein G

coupled to Sepharose (Amersham Biosciences) at 4ºC. Specific immunoprecipitations of the pre-cleared lysates were carried out in the presence of the appropriate antibody, coupled to protein G-Sepharose. After overnight incubation at 4ºC, immunoprecipitates were isolated by centrifugation and washed three times with lysis buffer. Precipitated proteins were separated by SDS-PAGE, electrotransferred to a PVDF membrane and immunodetected. Specific protein bands were revealed with the SuperSignal chemiluminescent substrate (Pierce).

Animals and Housing

Mice from the strain C57BL/6J of different ages (4, 32 and 60 weeks old), were obtained from The Jackson Laboratory (Bar Harbor, ME, USA). Their lungs were excised and snap frozen in liquid nitrogen for quantitative RT-PCR studies. Transgenic mice expressing human S-Endoglin under the control of the endothelial-specific promoter ICAM-2 (*S-Eng*$^+$ mice) have been previously described[14]. Briefly, transgenic mice were obtained by microinjection of the pICAM-2/S-Eng construct into fertilized C57Bl/6xSJL mouse embryos, and backcrossed at least five times with C57Bl/6 mice. Transgenic *S-Eng*$^+$ animals were genotyped using two sets of primers amplifying a 300-bp product for the endogenous mouse *endoglin*, and a 604-bp product for the transgene, as previously described[9]. Experiments were performed in parallel on *S-Eng*$^+$ mice and littermates that did not carry the transgene weighing 25-30 g at the time of radiotelemetry implant. Multiple simultaneous measurements were made with each mouse as indicated.

All procedures were approved by the Animal Care and Use Committees of the University of Salamanca and Instituto de Investigaciones Biomédicas Alberto Sols, and mice were cared for in accordance with the standards established in the National Institutes of Health *Guide for the Care and Use of Laboratory Animals*.

Direct Measurement of Blood Pressure: Radiotelemetry Methods

Arterial pressure was measured by telemetry in animals without anaesthesia or movement restriction, thus avoiding the confounding effects of anaesthesia and movement restriction on arterial pressure. Radiotelemetry system blood pressure measurement is performed through a

catheter implanted into an artery of the mouse. The catheter is attached to a combination pressure transducer, transmitter, and battery, all encapsulated in an implantable microminiaturized electronic monitor (PA-C20, Data Sciences International, DSI; St. Paul, MN). For device implantation in the mice, we have used the technique described by Whitesall et al. (2004)[15]. In brief, after anesthesia (Ketamin 78 $mg \cdot Kg^{-1}$, Diazepam 6 $mg \cdot Kg^{-1}$, and Atropine 0,15 $mg \cdot Kg^{-1}$; i.p.) a two skin incision were made, one 20-30 mm long from pelvis to xiphoid process and other in the neck from chin to manubrium. Then, a subcutaneous channel from the neck site to the abdominal site was made by blunt dissection and a 16-gauge trocar was passed from the abdominal to the neck incision. The catheter of the implant was passed into the trocar, and the implant body was inserted in the abdominal cavity through a midline incision made in the abdominal muscles and secured with six to eight interrupted nonabsorbable sutures (4-0 braided polyester). The muscle was closed with continuous sutures, the skin was closed with staples, and topical antiseptic was applied. Next, carotid artery was cannulated with the device's catheter and the skin was closed. Then, approximately 1 mL of normal saline was injected subcutaneously and the animal was kept in a warmed environment for at least 24 h to allow the recovering from surgery. An analgesic (buprenorphine, 0.1 $mg \cdot Kg^{-1}$ i.m., Buprex, Schering-Plough, Madrid, Spain) was provided if the animal behavior suggested the presence of pain. An antibiotic (cefazolin $25mg \cdot Kg^{-1}$, Normon, Spain) was administered at the time of the operation and twice daily during recovery. Each animal was housed individually in a standard polypropylene cage in a 12:12-h light-dark cycle, fed standard rodent chow, and given drinking water *ad libitum*. At least 3 days after recovery, the cage was placed over a radio receiver in a quiet environment, and repeated measurements of basal systolic and diastolic arterial pressure and heart rate were performed in each animal between 10:00 and 14:00 a.m., for at least 3 days. Responses of arterial pressure to intraperitoneal administration of L-NAME (50 $mg \cdot kg^{-1}$), acetylcholine ($1\mu g \cdot kg^{-1}$), hydralazine (0.2 $mg \cdot kg^{-1}$), nitroprusside (2 $mg \cdot kg^{-1}$) or TGF-β1 (5

μg.kg^{-1}) were also recorded in a similar way as basal data. Data was digitally recorder on a computer and processed using the software provided by Data Sciences.

When pressure measurement was finished, animals were anesthetized with a mixture of ketamine (100 mg·kg^{-1}) and xylazine (5 mg·kg^{-1}), the implant was removed and lungs and kidneys were immediately frozen in liquid nitrogen.

Biochemical measurements

For urinary nitrite measurements, mice were placed in metabolic cages and urine was collected free of food and faeces. Urinary nitrite concentration was measured using the Griess reactive, as previously described[16]. eNOS and COX-2 expression in extracts from kidneys and lungs was assessed as previously described[16]. Antibodies used were anti-eNOS (sc-654) and anti-COX-2 (sc-1745) both from Santa Cruz Biotechnology (Santa Cruz, CA, USA).

Statistics

All data are given as means ±SEM from at least three independent experiments. Statistical significance was evaluated using the Students' *t*-test. Differences were considered to be significant at a value of $P<0.05$.

REFERENCES

1. Blanco FJ, Santibanez JF, Guerrero-Esteo M, Langa C, Vary CP, Bernabeu C. Interaction and functional interplay between endoglin and ALK-1, two components of the endothelial transforming growth factor-beta receptor complex. *J Cell Physiol.* 2005;204:574-584.
2. Conley BA, Koleva R, Smith JD, Kacer D, Zhang D, Bernabeu C, Vary CP. Endoglin controls cell migration and composition of focal adhesions: function of the cytosolic domain. *J Biol Chem.* 2004;279:27440-27449.
3. Letamendia A, Lastres P, Botella LM, Raab U, Langa C, Velasco B, Attisano L, Bernabeu C. Role of endoglin in cellular responses to transforming growth factor-beta. A comparative study with betaglycan. *J Biol Chem.* 1998;273:33011-33019.
4. Ades EW, Candal FJ, Swerlick RA, George VG, Summers S, Bosse DC, Lawley TJ. HMEC-1: establishment of an immortalized human microvascular endothelial cell line. *J Invest Dermatol.* 1992;99:683-690.
5. Dimri GP, Lee X, Basile G, Acosta M, Scott G, Roskelley C, Medrano EE, Linskens M, Rubelj I, Pereira-Smith O, et al. A biomarker that identifies senescent human cells in culture and in aging skin in vivo. *Proc Natl Acad Sci U S A.* 1995;92:9363-9367.

6. Bellon T, Corbi A, Lastres P, Cales C, Cebrian M, Vera S, Cheifetz S, Massague J, Letarte M, Bernabeu C. Identification and expression of two forms of the human transforming growth factor-beta-binding protein endoglin with distinct cytoplasmic regions. *Eur J Immunol.* 1993;23:2340-2345.

7. Pérez-Gómez E, Villa-Morales M, Santos J, Fernández-Piqueras J, Gamallo C, Dotor J, Bernabéu C, Quintanilla M. A role for endoglin as a suppressor of malignancy during mouse skin carcinogenesis. *Cancer Res.* 2007;67:10268-10277.

8. Guerrero-Esteo M, Sanchez-Elsner T, Letamendia A, Bernabeu C. Extracellular and cytoplasmic domains of endoglin interact with the transforming growth factor-beta receptors I and II. *J Biol Chem.* 2002;277:29197-29209.

9. Perez-Gomez E, Eleno N, Lopez-Novoa JM, Ramirez JR, Velasco B, Letarte M, Bernabeu C, Quintanilla M. Characterization of murine S-endoglin isoform and its effects on tumor development. *Oncogene.* 2005;24:4450-4461.

10. Dennler S, Itoh S, Vivien D, ten Dijke P, Huet S, Gauthier JM. Direct binding of Smad3 and Smad4 to critical TGF beta-inducible elements in the promoter of human plasminogen activator inhibitor-type 1 gene. *EMBO J.* 1998;17:3091-3100.

11. Korchynskyi O, ten Dijke P. Identification and functional characterization of distinct critically important bone morphogenetic protein-specific response elements in the Id1 promoter. *J Biol Chem.* 2002;277:4883-4891.

12. van Zonneveld AJ, Curriden SA, Loskutoff DJ. Type 1 plasminogen activator inhibitor gene: functional analysis and glucocorticoid regulation of its promoter. *Proc Natl Acad Sci U S A.* 1988;85:5525-5529.

13. Tournay O, Benezra R. Transcription of the dominant-negative helix-loop-helix protein Id1 is regulated by a protein complex containing the immediate-early response gene Egr-1. *Mol Cell Biol.* 1996;16:2418-2430.

14. Velasco B, Ramirez JR, Relloso M, Li C, Kumar S, Lopez-Bote JP, Perez-Barriocanal F, Lopez-Novoa JM, Cowan PJ, d'Apice AJ, Bernabeu C. Vascular gene transfer driven by endoglin and ICAM-2 endothelial-specific promoters. *Gene Ther.* 2001;8:897-904.

15. Whitesall SE, Hoff JB, Vollmer AP, D'Alecy LG. Comparison of simultaneous measurement of mouse systolic arterial blood pressure by radiotelemetry and tail-cuff methods. *Am J Physiol Heart Circ Physiol.* 2004;286:H2408-2415.

16. Jerkic M, Rivas-Elena JV, Prieto M, Carron R, Sanz-Rodriguez F, Perez-Barriocanal F, Rodriguez-Barbero A, Bernabeu C, Lopez-Novoa JM. Endoglin regulates nitric oxide-dependent vasodilatation. *FASEB J.* 2004;18:609-611.

17. Jerkic M, Rivas-Elena JV, Santibanez JF, Prieto M, Rodriguez-Barbero A, Perez-Barriocanal F, Pericacho M, Arevalo M, Vary CP, Letarte M, Bernabeu C, Lopez-Novoa JM. Endoglin regulates cyclooxygenase-2 expression and activity. *Circ Res.* 2006;99:248-256.

Specific Primers used for RT-PCR

	Target	Sequence (5' → 3') Forward	Reverse
#1	Endoglin- CT (human)	GAATTCTGGTACATCTACTCGC	GGCTATGCCATGCTGCTGGTGG
#2	ALK-1 (human)	GCAGATCTGACCCTGTGAAGCCG	TACCGCGGCTGGCCATCTGTTCC
#3	ALK-5 (human)	GGCCATGGATCTGCCACAACC	GACCCGGGTACATTTTGATGCC
#4	TβR-II (human)	ATGGCCATGGAGGCCCGCGTTAACCGGCAG	GAGGATCCTATTTGGTAGTGTTTAG
#5	hTERT (human)	CGTGGTTTCTGTGTGGTGTC	AGAGGAAGTGCTTGGTCTCG
#6	Id1 (human)	GGTGCGCTGTCTGTCTGAG	TAGTCGATGACGTGCTGGAG
#7	PAI-1 (human)	CTCTCTCTGCCCTCACCAAC	GTGGAGAGGCTCTTGGTCTG
#8	GAPDH (human)	GGCTGAGAACGGGAAGCTTGTCA	CGGCCATCACGCCACACAGT
#9	S-Endoglin (mouse)	GCCTTGTCCTGCCCTCTGTA	TGGGAATGGGGTGGAGGCTT
#10	18S RNA (mouse)	CCAGTAAGTGCGGGTCATAAGC	CCTCACTAAACCATCCAATCGG

Online Table I. Nucleotide sequences of specific primers used to amplify L-Endoglin, S-Endoglin, ALK1, ALK5, TβR-II, human telomerase reverse transcriptase (hTERT), Id1, PAI-1, 18S RNA and GAPDH transcripts by PCR. Human Endoglin cytoplasmic (Endoglin-CT) primers #1 simultaneously detect the cytoplasmic (CT) regions of L-Endoglin (150-bp) and S-Endoglin (285-pb) isoforms. Mouse endoglin primers #6 detect the S-Endoglin isoform.

Treatment		Group	(n)	Absolute values (mmHg) Before	Absolute values (mmHg) After	Net changes (mmHg)	Relative changes (%)
None	Systolic pressure	Eng+	(83)	135 ± 2			
		WT	(75)	108 ± 2*			
	Diastolic pressure	Eng+	(83)	105 ± 2			
		WT	(75)	87 ± 2*			
Acetilcholine (1 μg·kg^{-1})	Systolic pressure	Eng+	(20)	131 ± 3	122 ± 3	-9 ± 2	-6.8 ± 0.2
		WT	(15)	105 ± 3*	95 ± 5*	-10 ± 2	-9.5 ± 0.3*
	Diastolic pressure	Eng+	(20)	112 ± 2	104 ± 4	-8 ± 2	-7.1 ± 0.3
		WT	(15)	87 ± 3*	75 ± 5*	-12 ± 2	-13.7 ± 0.3*
L-NAME (50 mg·kg^{-1})	Systolic pressure	Eng+	(30)	137 ± 3	151 ± 3	23 ± 2	16.7 ± 0.78
		WT	(22)	107 ± 4*	141 ± 5	34 ± 2*	31.2 ± 0.9*
	Diastolic pressure	Eng+	(30)	108 ± 3	127 ± 3	19 ± 2	17.5 ± 0.7
		WT	(22)	83 ± 4*	116 ± 4	33 ± 2	38.3 ± 1.0*
Hydralazine (0.2 mg·kg^{-1})	Systolic pressure	Eng+	(10)	144 ± 4	110 ± 5	-34 ± 4	-23.6 ± 2.7
		WT	(10)	113 ± 6*	78 ± 6*	-35 ± 4	-30.7 ± 3.9
	Diastolic pressure	Eng+	(10)	117 ± 4	91 ± 3	-26± 2	-22.2 ± 2.7
		WT	(10)	87 ± 6*	57 ± 4*	-30 ± 4	-34.4 ± 3.4*
Nitroprusside (2 mg·kg^{-1})	Systolic pressure	Eng+	(23)	135 ± 3	77 ± 3	-58 ± 7	-42.9 ± 4.7
		WT	(18)	113 ± 5*	78 ± 4	-55 ± 6	-51.7 ± 5.9
	Diastolic pressure	Eng+	(23)	105 ± 2	55 ± 6	-50 ± 2	-47.6 ± 5.7
		WT	(18)	88 ± 4*	37 ± 5*	-52 ± 4	-59.0 ± 3.4*
TGF-β1 (5 μg·kg^{-1})	Systolic pressure	Eng+	(10)	131 ± 3	122 ± 12	-9 ± 2	- 6.8 ± 0.2
		WT	(10)	105 ± 4*	88 ± 19*	-17 ± 2*	-10.5 ± 0.4*
	Diastolic pressure	Eng+	(10)	106 ± 3	99 ± 6	-7 ± 2	- 6.6 ± 0.4
		WT	(10)	88 ± 5*	73 ± 5*	-15 ± 2*	-17.5 ± 0.7*

Online Table II. Hemodynamic values in transgenic mice expressing S-Endoglin (*P<0.01).

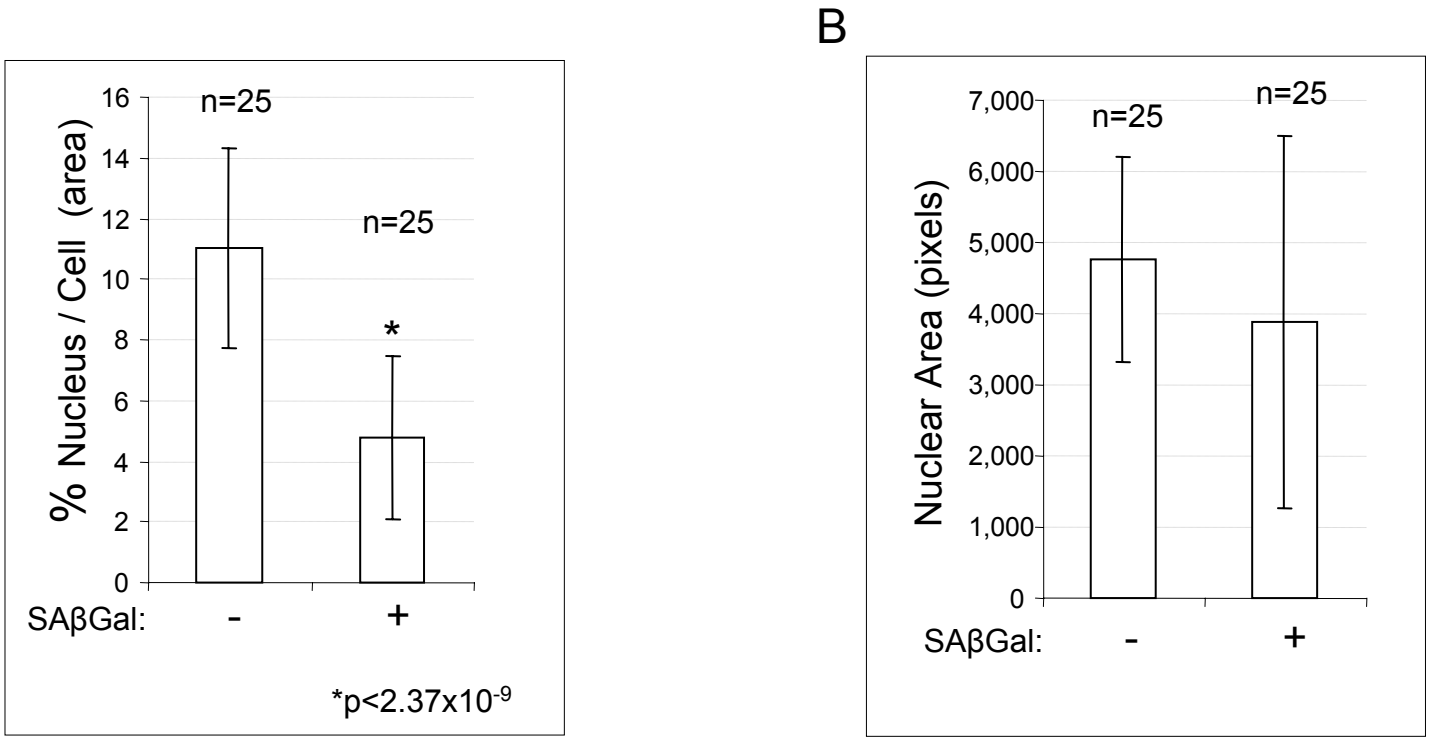

Online Figure I. Cell size analysis of SA-β-gal positive endothelial cells. HUVECs were seeded onto gelatin coated plates and passages were performed when cells achieved ~90% confluence. At passages 12-14, cells were stained for SA-β-gal activity. Blue cytoplasmic staining in cells positive for SA-β-gal was considered as a marker for senescent cells. The percentage that the nuclear area represents respect to the whole cell was measured in senescent and non-senescent cells from at least four random fields and was represented as the mean ±SD (panel A). The nuclear area (in pixels) of senescent and non-senescent cells was measured in at least four random fields and represented as the mean ±SD (panel B). This is a representative experiment out of three different ones. The surface ratio Nucleus/Cell is significantly much lower in senescent versus non-senescent cells (*$p<2.37x10^{-9}$). As a control, no significant differences (NS) were observed in the nuclear area between senescent and non-senescent cells.

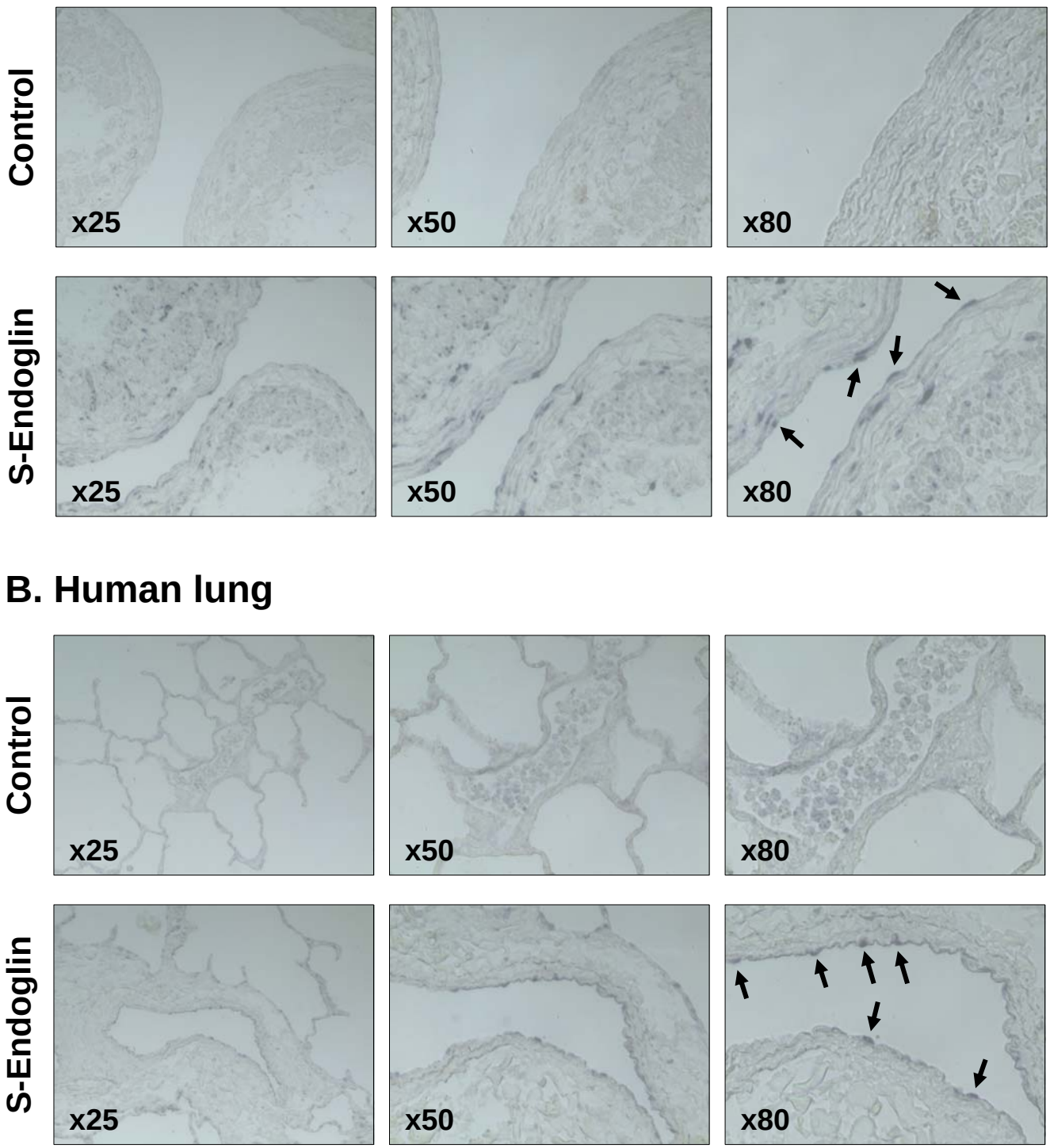

Online Figure II. In situ hybridization of S-Endoglin in human veins and lung. Sense (Control) and antisense S-Endoglin cRNA probes were uniformly labeled with digoxigenin-UTP and hybridized to slides from human coronary artery. Riboprobes were detected with anti-digoxigenin Fab fragments conjugated to alkaline phosphatase, followed by incubation with the chromogenic substrate. No contrast staining was performed. Slides were photographed at the indicated magnifications. Black arrows show the specific hybridization of S-Endoglin to the endothelium.

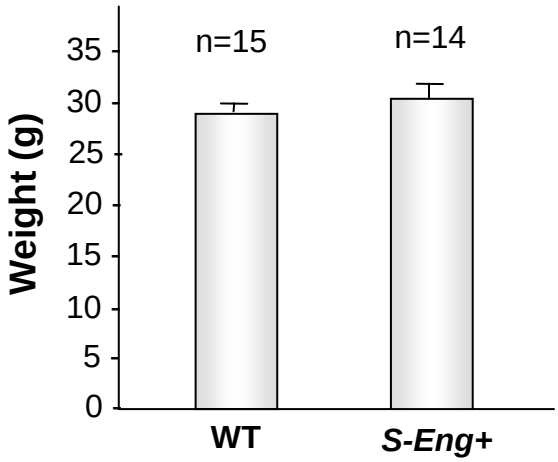

Online Figure III. Weight in wild type (WT; n=15) and *S-Endoglin*$^{+}$ (n=14) mice was determined.